

University of Groningen

## Characterization of a thermostable flavin-containing monooxygenase from *Nitricola lacsaponensis* (NiFMO)

Lončar, Nikola; Fiorentini, Filippo; Bailleul, Gautier; Savino, Simone; Romero, Elvira; Mattevi, Andrea; Fraaije, Marco W

*Published in:*  
Applied Microbiology and Biotechnology

*DOI:*  
[10.1007/s00253-018-09579-w](https://doi.org/10.1007/s00253-018-09579-w)

**IMPORTANT NOTE: You are advised to consult the publisher's version (publisher's PDF) if you wish to cite from it. Please check the document version below.**

*Document Version*  
Publisher's PDF, also known as Version of record

*Publication date:*  
2019

[Link to publication in University of Groningen/UMCG research database](#)

### *Citation for published version (APA):*

Lončar, N., Fiorentini, F., Bailleul, G., Savino, S., Romero, E., Mattevi, A., & Fraaije, M. W. (2019). Characterization of a thermostable flavin-containing monooxygenase from *Nitricola lacsaponensis* (NiFMO). *Applied Microbiology and Biotechnology*, 103(4), 1755-1764. <https://doi.org/10.1007/s00253-018-09579-w>

### **Copyright**

Other than for strictly personal use, it is not permitted to download or to forward/distribute the text or part of it without the consent of the author(s) and/or copyright holder(s), unless the work is under an open content license (like Creative Commons).

The publication may also be distributed here under the terms of Article 25fa of the Dutch Copyright Act, indicated by the "Taverne" license. More information can be found on the University of Groningen website: <https://www.rug.nl/library/open-access/self-archiving-pure/taverne-amendment>.

### **Take-down policy**

If you believe that this document breaches copyright please contact us providing details, and we will remove access to the work immediately and investigate your claim.

Downloaded from the University of Groningen/UMCG research database (Pure): <http://www.rug.nl/research/portal>. For technical reasons the number of authors shown on this cover page is limited to 10 maximum.



# Characterization of a thermostable flavin-containing monooxygenase from *Nitriicola lacisaponensis* (NiFMO)

Nikola Lončar<sup>1,2</sup> · Filippo Fiorentini<sup>3</sup> · Gautier Bailleul<sup>2</sup> · Simone Savino<sup>2,3</sup> · Elvira Romero<sup>2</sup> · Andrea Mattevi<sup>3</sup> · Marco W. Fraaije<sup>1,2</sup>

Received: 3 October 2018 / Revised: 6 December 2018 / Accepted: 11 December 2018 / Published online: 4 January 2019  
© Springer-Verlag GmbH Germany, part of Springer Nature 2019

## Abstract

The flavin-containing monooxygenases (FMOs) play an important role in drug metabolism but they also have a high potential in industrial biotransformations. Among the hitherto characterized FMOs, there was no thermostable representative, while such biocatalyst would be valuable for FMO-based applications. Through a targeted genome mining approach, we have identified a gene encoding for a putative FMO from *Nitriicola lacisaponensis*, an alkaliphilic extremophile bacterium. Herein, we report the biochemical and structural characterization of this newly discovered bacterial FMO (NiFMO). NiFMO can be expressed as active and soluble enzyme at high level in *Escherichia coli* (90–100 mg/L of culture). NiFMO is relatively thermostable (melting temperature ( $T_m$ ) of 51 °C), displays high organic solvent tolerance, and accepts a broad range of substrates. The crystal structure of NiFMO was solved at 1.8 Å resolution, which allows future structure-based enzyme engineering. Altogether, NiFMO represents an interesting newly discovered enzyme with the appropriate features to develop into an industrially applied biocatalyst.

**Keywords** Monooxygenase · Thermostability · Indigo bioproduction

## Introduction

Mammalian FMOs are well-known monotopic membrane enzymes involved in the oxidation of xenobiotics and have been extensively studied for their contribution in phase-I metabolic processes (Cashman and Zhang 2006; Krueger and Williams 2005; Phillips and Shephard 2016). The original interest for the roles of these oxidative flavoenzymes in drug metabolism has been quickly matched by an equally strong appeal for their potential in biotransformations (Choi et al. 2003; Han et al.

2011; Rioz-Martínez et al. 2011). Besides the exploitation of soluble microbial homologs as mimics of mammalian FMOs for the enantioselective preparation of drug metabolites (Gul et al. 2016), bacterial variants have also shown promise for the bioproduction of indigo and indigo derivatives, which can be very valuable both as dyes and as precursors of pharmaceuticals (Ameria et al. 2018; Choi et al. 2003; Han et al. 2011; Hsu et al. 2018). A designed metabolic pathway which involves a bacterial FMO for the hydroxylation of indole has been recently developed and allows a new dyeing strategy. Such FMO-based biotechnological process would offer a green alternative to the classic and highly polluting indigo dyeing process (Hsu et al. 2018).

Although microbial FMOs are generally expressed in good amounts in convenient heterologous systems such as *Escherichia coli*, all characterized FMOs have not shown a very high thermal stability, a key requisite for industrial applications (Alfieri et al. 2008; Orru et al. 2010). For this reason, we have been seeking for more stable FMOs through screening of the sequenced microbial genomes. Our search led us to identify a gene encoding for a putative FMO present in *Nitriicola lacisaponensis*, an alkaliphilic bacterium isolated from the Soap Lake, an alkaline (pH ~9.8) and saline (NaCl ~10% w/v) lake

---

Nikola Lončar and Filippo Fiorentini contributed equally to this work.

✉ Andrea Mattevi  
andrea.mattevi@unipv.it

✉ Marco W. Fraaije  
m.w.fraaije@rug.nl

<sup>1</sup> Groningen Enzyme and Cofactor Collection (GECCO), University of Groningen, Nijenborgh 4, 9747AG Groningen, The Netherlands

<sup>2</sup> Molecular Enzymology Group, University of Groningen, Nijenborgh 4, 9747AG Groningen, The Netherlands

<sup>3</sup> Structural Biology Lab, Department of Biology and Biotechnology “L. Spallanzani”, University of Pavia, Via Ferrata 9, 27100 Pavia, Italy

located in Grant County, USA (Dimitriu et al. 2005). Here, we report the biochemical and structural characterization of this novel bacterial FMO (NiFMO), which was found to display high thermostability, organic solvent tolerance, and a broad substrate profile. The robustness of this newly discovered FMO makes it an attractive biocatalyst for selective oxygenation reactions.

## Materials and methods

### Chemicals and reagents

Bovine liver catalase, indigo, indole, and indole derivatives were purchased from Sigma-Aldrich. All other chemicals were analytical grade and obtained from Sigma-Aldrich or Merck. NADPH and NADP<sup>+</sup> were purchased from Oriental Yeast Co. LTD.

### Strains, plasmids, and growth conditions

A codon-optimized gene (GenBank accession number MK061530) encoding NiFMO (GenBank: WP\_036542404.1) for *E. coli* expression was synthesized by GenScript. Using restriction cloning, the gene was cloned into a pBAD vector resulting in two constructs for expressing NiFMO with an N-terminal fusion partner: (a) NiFMO fused to His<sub>6</sub>-SUMO (SUMO = small ubiquitin-like modifier) and (b) NiFMO fused to His-tagged phosphite dehydrogenase (His<sub>6</sub>-PTDH). Primers and plasmid maps are available upon request. Plasmid sequences were verified by sequencing (Eurofins Genomics). Recombinant His<sub>6</sub>-SUMO-NiFMO and His<sub>6</sub>-PTDH-NiFMO were overexpressed and purified according to the following procedure; *E. coli* NEB10β cells were freshly transformed with the corresponding plasmid and an overnight culture was diluted 100-fold into 400 mL Terrific Broth medium with 50 μg/mL ampicillin (TB<sub>amp</sub>) in 2-L baffled flasks. Cells were induced at OD<sub>600</sub> = 1.5 with 0.02% w/v L-arabinose (final concentration) and incubated at 25 °C for 36 h (135 rpm). Cells were harvested at 4 °C and centrifuged at 6000 rpm using JA10.500 rotor for 20 min in the Beckman-Coulter centrifuge. They were then washed and resuspended in 50 mM potassium phosphate (KPi) buffer pH 7.5 containing 0.25 M NaCl and 0.1 mM phenylmethylsulfonyl fluoride. Resuspended cells were disrupted by sonication and centrifuged at 4 °C 16000 rpm using JA17 rotor for 45 min. The cell-free extract was applied on a 5 mL HiTrap Ni-Sepharose HP column pre-equilibrated in 50 mM KPi buffer pH 7.5 with 0.25 M NaCl. Stepwise elution was used to wash non-specifically bound proteins and elution of NiFMO

was achieved with 50 mM KPi buffer pH 8.0, 0.25 M NaCl, and 500 mM imidazole. After SDS-PAGE analysis, pure fractions were pooled, buffer exchanged to 50 mM KPi pH 7.5, and flash frozen in liquid nitrogen. Samples were stored at −20 °C until further use. Concentration of purified NiFMO fusions was determined by using an extinction coefficient of 15.0 mM<sup>−1</sup> cm<sup>−1</sup> at 440 nm. Extinction coefficient was determined as described previously (Aliverti et al. 1999).

### Thermal stability assays

The ThermoFAD method (Forneris et al. 2009) was used to determine the apparent melting temperature of His<sub>6</sub>-PTDH-NiFMO in different pH conditions or in the presence of additives. By means of an RT-PCR machine (CFX96-Touch, Bio-Rad), the fluorescence of the FAD cofactor was monitored using a 450–490 excitation filter and a 515–530 nm emission filter, typically used for SYBR Green based RT-PCR. The temperature was increased with 0.5 °C per step, starting at 25 °C and ending at 90 °C, using a holding time of 10 s at each step. The maximum of the first derivative of the observed flavin fluorescence was taken as the apparent melting temperature. Twenty microliter of the enzyme solution containing 10 μM His<sub>6</sub>-PTDH-NiFMO and the additive (solvent or buffer of appropriate pH) was put into a 96 wells PCR plate and covered with a transparent adhesive film.

### Steady-state kinetic analysis

Kinetic assays were performed in duplicates for 120 s using a Jasco V-660 spectrophotometer and H1MD microplate reader (BioTek). Different concentrations of substrates (0.05–2.50 mM) were dissolved in 50 mM KPi pH 7.5. Stock solutions of indole derivatives (indoline, pyrrole, and 6-Br-indole) were prepared in methanol. The final concentration of methanol in the test reaction was kept below 1% (v/v). His<sub>6</sub>-PTDH-NiFMO (final concentration 0.5 μM) was added to the reaction mixture and the reaction was started by the addition of 0.10 mM NADPH (final concentration). NADPH consumption was followed at 340 nm.

### pH optimum and activity in presence of co-solvents

Determination of the pH optimum of His<sub>6</sub>-PTDH-NiFMO activity was performed by using the above described procedures with a series of 50 mM buffers (sodium-acetate pH 4.0–5.6, KPi pH 5.8–8.0, tris(hydroxymethyl)aminomethane-HCl pH 7.5–9.0). Final concentrations in the reaction mixtures were 1.0 mM trimethylamine, 1.0 μM His<sub>6</sub>-PTDH-NiFMO, and 0.10 mM NADPH.

## Rapid kinetics analysis

The stopped flow experiments were carried out using NiFMO fused to His<sub>6</sub>-SUMO. The reaction of NiFMO with dioxygen was studied using the single-mixing mode of a SX20 stopped flow spectrophotometer equipped with a photodiode array detector (Applied Photophysics, Surrey, UK). All solutions were prepared in 50 mM KPi pH 7.5. Reactions were run in duplicate by mixing equal volumes of two solutions, at 25 °C. The stopped flow instrument was made anaerobic by flushing the flow-circuit with a dioxygen-scrubbing solution containing 5.0 mM glucose and 0.3 μM glucose oxidase (*Aspergillus niger*, type VII, Sigma-Aldrich). To prepare fully reduced NiFMO, titrations of oxidized NiFMO with NADPH were carried out in a vial under anaerobic conditions. After adding a small aliquot (< 10 μL) of NADPH (> 40 mM) to the enzyme (15–30 μM), the mixture was incubated at room temperature until no further enzyme reduction was observed. The titration was then continued until NiFMO was completely reduced as evidenced by the bleaching of the flavin. The resulting reduced enzyme was loaded into the stopped flow instrument and mixed with buffer containing various dioxygen concentrations to monitor the spectral changes taking place in the stopped flow cell. To achieve the desired final dioxygen concentration (0.13, 0.31, 0.61, and 0.96 mM), the anaerobic enzyme solution was mixed with (i) air-saturated buffer; (ii) solution containing equal amounts of buffer bubbled with 100% nitrogen and buffer bubbled with 100% dioxygen; (iii) buffer bubbled with 100% dioxygen; and (iv) buffer bubbled with 100% dioxygen in ice. The bubbling time for all solutions was 10 min. The lowest dioxygen concentration was assayed in the presence and the absence of trimethylamine (150 μM final concentration). The stopped flow traces at 359 and 440 nm were fit to exponential functions to determine the observed rates ( $k_{\text{obs}}$ ). The second-order rate constant for the reaction of the reduced flavin with dioxygen was calculated from the slope of the linear plot of  $k_{\text{obs}}$  versus dioxygen concentration. All data were analyzed using the software Pro-Data (Applied Photophysics, Surrey, UK) or GraphPad Prism 6.05 (La Jolla, CA, USA).

## Crystallization of NiFMO

After His<sub>6</sub>-SUMO tag cleavage using SUMO protease and elution of the unbound native NiFMO from a second His-trap column, the protein was further purified and oligomeric state was analyzed by size-exclusion chromatography (Superdex 200 10/300, GE Healthcare). The eluted peak was concentrated up to 12 mg/mL and used for crystallization trials (final buffer composition 25 mM tris(hydroxymethyl)aminomethane-HCl pH 8.0, 200 mM NaCl). NADP<sup>+</sup> (1.0 mM final concentration) was added to the protein solution immediately before

crystallization experiments. The crystallization screening was performed by means of an Oryx 8 crystallization robot (Douglas Instruments). NiFMO crystallized in 0.20 M Mg formate and 20% (w/v) PEG3350 at 4 °C in micro-batch configuration.

## X-ray methods

The crystal structure of NiFMO was solved using standard methods. Diffraction data measured at 100 K on the beam line PX-III of the Swiss Light Source (Villigen, CH). Data were processed with XDS and programs of the CCP4 suite (Kabsch 2010; Winn et al. 2011). The structure was solved by molecular replacement using the PDB entry 2VQ7 (Alferi et al. 2008) as search model and the program Phaser (McCoy et al. 2007). The structure was refined at 1.8 Å resolution using Refmac5 and Coot (Dodson et al. 1996; Emsley and Cowtan 2004). Crystallographic statistics are listed in Table 1. Model analysis was done with Coot (Emsley and Cowtan 2004), PISA (Krissinel and Henrick 2007), and ESBRI (Costantini et al. 2008).

**Table 1** Crystallographic table for the structure of the wild-type NiFMO in complex with NADP<sup>+</sup>

PDB code	6HNS
Resolution range	50–1.84
Space group	P2 <sub>1</sub> 2 <sub>2</sub> 1
Unit cell (Å)	59.06, 125.61, 144.72
Total reflections	413,067 (19305)
Unique reflections	93,414 (4431)
Multiplicity	4.4 (4.4)
Completeness (%)	99.2 (97.1)
Mean I/sigma (I)	14.7 (1.6)
R-merge (%)	0.076 (0.849)
CC1/2 <sup>a</sup>	0.99 (0.58)
R-work (%)	0.191
R-free (%)	0.222
Number of non-hydrogen atoms	
Protein	7227
Ligands (FAD/NADP <sup>+</sup> /Mg <sup>++</sup> )	204
Waters	465
RMS (bonds) (Å)	0.011
RMS (angles) (°)	1.61
Ramachandran favored (%)	96
Ramachandran allowed (%)	4
Ramachandran outliers (%)	0
Average B-factor (Å <sup>2</sup> )	26.0

<sup>a</sup> Statistics for the highest-resolution shell are shown in parentheses

<sup>b</sup> A cutoff criterion for resolution limits was applied on the basis of the mean intensity correlation coefficient of half-subsets of each dataset

## Results

### Substrate acceptance profile and thermostability of NiFMO

NiFMO could be expressed in excellent amounts in *E. coli*. Using affinity chromatography, the enzymes could be isolated in high yields 90–100 mg of purified protein per liter of culture broth (Fig. 1a). The His<sub>6</sub>-PTDH-NiFMO was used for biochemical and biocatalytic exploration while the His<sub>6</sub>-SUMO-NiFMO was used for crystallization purposes after cleavage of the tag. From gel permeation analysis, the wild-type NiFMO proved to behave as a functional dimer ( $2 \times 53$  kDa), containing one molecule of non-covalently tightly bound FAD per monomer (Fig. 1). This is similar to FMO from *Methylophaga* sp. (Alfieri et al. 2008). To establish whether NiFMO can be used for selective oxygenation, several potential substrates were tested. In the first experiments, it was found that already without adding a potential substrate an appreciable rate of NADPH oxidation was observed ( $\sim 0.1$  s<sup>-1</sup>). The rate for uncoupling is normally lower for FMOs or related class B flavoprotein monooxygenases (van Berkel et al. 2006). Soon, it was realized that NiFMO also accepts the used buffer, tris(hydroxymethyl)aminomethane, as a substrate. By changing to a phosphate buffer, the rate of uncoupling (NADPH oxidation in the absence of any substrate) could be determined: 0.015 s<sup>-1</sup>. Next, the steady-state kinetic parameters were determined for several substrates (Table 2). While tris(hydroxymethyl)aminomethane was a poor substrate in terms of kinetic parameters when compared with the other compounds, the  $K_M$  value of 21.5 mM turned out fall in the range of the concentrations initially used in the experiments. This fully explains the interference of tris(hydroxymethyl)aminomethane when measuring activity of other test compounds.

The substrates display rather similar  $k_{cat}$  values (0.09–2.01 s<sup>-1</sup>) while the  $K_M$  values vary somewhat more (45.6–21,500  $\mu$ M). Trimethylamine and methimazole are the

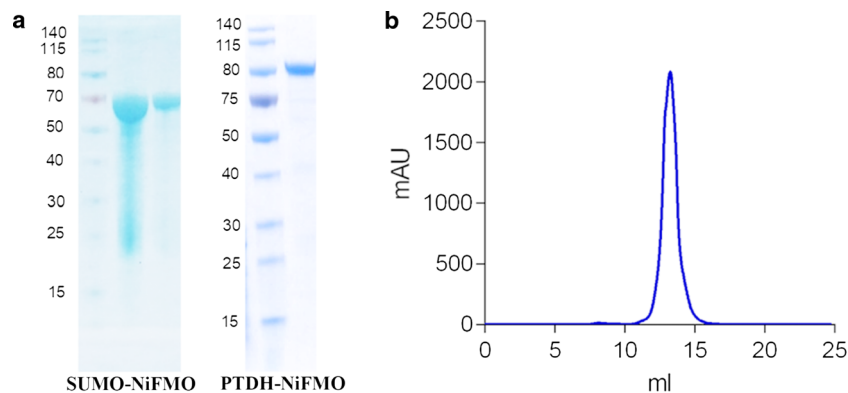
best substrates when considering the kinetic parameters. Yet, also more bulky compounds, such as indole, 6-bromoindole, and indoline are accepted by the enzyme. In particular, indigo conversion could be easily observed by the appearance of a blue color indicating the formation of indigo blue. All abovementioned reactions were measured using 100  $\mu$ M NADPH. NADH was not accepted by the enzyme as coenzyme. Using 3.0 mM trimethylamine as saturating substrate, the  $K_M$  for NADPH was determined: 8.2  $\mu$ M.

The activity and stability of the enzyme was evaluated at different pH values and co-solvent conditions both by means of checking the NADPH depletion rates in the presence of trimethylamine, and by detecting the apparent melting temperature using the ThermoFAD method (Forneris et al. 2009). The effects of pH and co-solvents on NiFMO activity and the apparent melting temperature are shown in Fig. 2. The optimal pH for activity was found to be slightly basic, between pH 7 and 8. Also, the thermostability (highest  $T_m$  of 51 °C) was highest at slightly alkaline conditions. The solvent tolerance of NiFMO proved to be rather good as the enzyme retains activity even in the presence of up to 10% solvent content. Specifically, high conversion rates were observed with methanol and acetonitrile as co-solvents. However, acetonitrile had a detrimental effect on the  $T_m$  of NiFMO, whereas the enzyme showed high thermostability ( $T_m \sim 47$  °C) in the presence of up to 10% (v/v) DMSO (Fig. 2c, d).

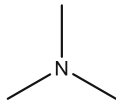
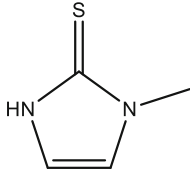
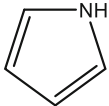
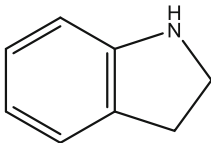
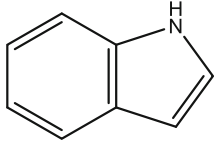
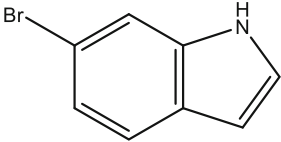
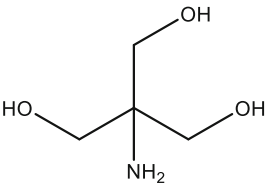
### Rapid kinetics assays reveal formation and stabilization of the C4a-hydroperoxyflavin intermediate

After identification of a set of compounds oxygenated by NiFMO (Fig. 3), we sought to investigate the oxidative half-reaction in the presence and absence of a suitable substrate, trimethylamine, by using the stopped flow technique. We initially monitored the spectral changes

**Fig. 1** Purification of NiFMO. On the left, a SDS-PAGE gel shows purified samples of His<sub>6</sub>-SUMO-tagged and His<sub>6</sub>-PTDH-tagged NiFMO. On the right, gel-filtration analysis of purified tag-free NiFMO is shown. The wild-type enzyme elutes as a monodispersed peak corresponding to a MW of  $\sim 100$  kDa, suggesting that NiFMO exists as a dimer in solution



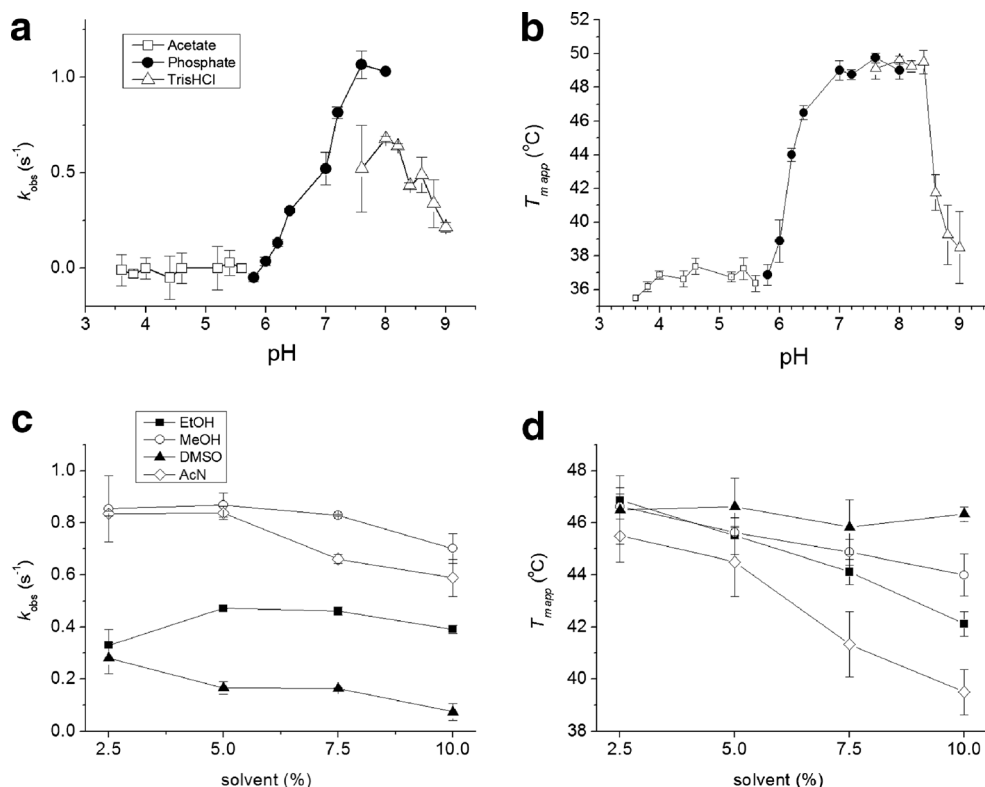
**Table 2** Steady-state kinetics of PTDH-NiFMO

		$k_{\text{cat}}$ ( $\text{s}^{-1}$ )	$K_{\text{M}}$ ( $\mu\text{M}$ )	$k_{\text{cat}}/K_{\text{M}}$ ( $\text{s}^{-1} \text{M}^{-1}$ )
Trimethylamine		$2.01 \pm 0.08$	$45.6 \pm 9.6$	44,000
Methimazole		$1.10 \pm 0.08$	$77 \pm 10$	14,000
Pyrrole		$0.69 \pm 0.03$	$146 \pm 17$	4,800
Indoline		$0.70 \pm 0.03$	$98 \pm 14$	7,100
Indole		$0.11 \pm 0.01$	$137 \pm 23$	730
6-Bromoindole		$0.09 \pm 0.03$	$640 \pm 340$	140
Tris(hydroxymethyl)aminomethane (TRIS)		$0.18 \pm 0.02$	$21500 \pm 5600$	9

occurring after mixing the fully NADPH-reduced NiFMO with various dioxygen concentrations, at pH 7.5 and 25 °C. In the absence of substrates, the fully reduced NiFMO reacted very rapidly with dioxygen to form a C4a-hydroperoxyflavin intermediate with an absorption maximum of 359 nm ( $80 \text{ s}^{-1}$ , at 0.13 mM dioxygen) (Fig. 4a, b). The observed rates for these reactions correlated linearly with the dioxygen concentration, giving a second-order rate constant for the reaction with dioxygen of  $0.4 \times 10^6 \text{ M}^{-1} \text{ s}^{-1}$  (Fig. 4a, inset). The intermediate slowly converted into fully oxidized NiFMO in the absence of trimethylamine ( $0.002\text{--}0.02 \text{ s}^{-1}$ ). Recovery of only 28% of the absorbance expected for the fully re-oxidized

enzyme was observed after 60 s (Fig. 4a). This slow recovery of the oxidized enzyme is fully in line with the observed slow uncoupling rate of  $0.015 \text{ s}^{-1}$ . We then tested the effect of trimethylamine on the enzyme re-oxidation in the presence of 0.13 mM dioxygen as co-substrate. In the presence of trimethylamine, the rate of formation of the intermediate was fast ( $100 \text{ s}^{-1}$ ). Enzyme re-oxidation was complete within 10 s when trimethylamine is included in the assays (Fig. 4c, d). The stopped flow traces at 440 nm for enzyme re-oxidation were best fit to a double exponential function, with an initial fast phase accounting for 87% of the total absorption change ( $4\text{--}9$  and  $6 \text{ s}^{-1}$ ).

**Fig. 2** Stability and co-solvent tolerance of NiFMO. Effect of the pH (a, b) and co-solvents (c, d) on NiFMO activity on trimethylamine (measured by NADPH depletion) and on the apparent melting temperature ( $T_{m,app}$ ) of NiFMO (measured by ThermoFAD technique). EtOH is ethanol, MeOH is methanol, and AcN is acetonitrile



## Crystal structure of NiFMO

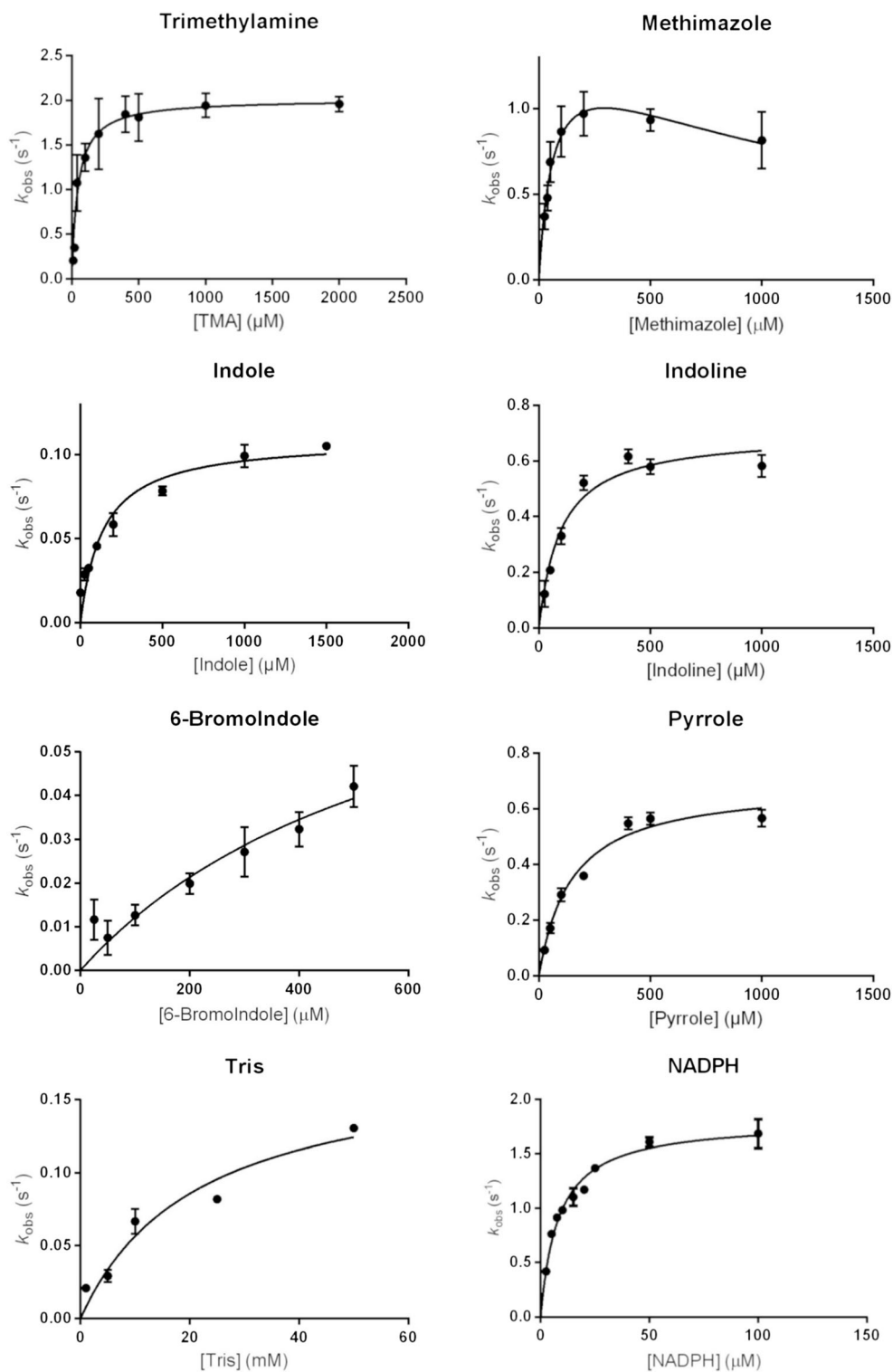
To correlate the biochemical profile of this novel bacterial FMO with the structural features, the tag-free purified protein was used for crystallization trials. Crystals were obtained only following incubation of the protein with 1.0 mM NADP<sup>+</sup>. The NiFMO structure was solved at 1.8 Å resolution by molecular replacement, resulting in an electron density of excellent quality (Fig. 5 and Table 1). In terms of overall structure, NiFMO is very similar to FMO from *Methylophaga* sp. strain SK1 (Alfieri et al. 2008), featuring two distinct domains for the binding of the nucleotide cofactors, FAD and NADP<sup>+</sup>, connected through a double linker. The sequence identity between the two proteins is 74% with a root-mean-square deviation of 0.4 Å between the C $\alpha$  atoms of the two proteins. The identity and the position of the catalytic residues shaping the active site are fully conserved, in agreement with the very similar substrate profiles of these bacterial FMOs. The oxygenation of indole and indole derivatives—a prerogative of bacterial FMO variants—was shown to correlate with the presence of a highly conserved tyrosine (Tyr207 in NiFMO) which positions as a front door leading suitable compounds to the oxygenating FAD intermediate. Its substitution to asparagine in mammalian FMOs results in a drastically decreased oxygenation of indigoid compounds

(Cho et al. 2011). The Tyr side chain may favor binding and correct positioning of the indigo-like substrates through favorable aromatic stacking interactions with the indigo aromatic ring (Fig. 6).

## Discussion

The bacterial FMOs characterized so far displayed substrate profiles very similar to the ones reported for human FMOs, which—with the exception of FMO5—are known to catalyze the oxygenation of different compounds bearing soft-nucleophilic heteroatoms, mainly *N*- and *S*-atoms (Cashman 2005; Fiorentini et al. 2016; Krueger and Williams 2005). The solubility and generally higher stability of the bacterial FMOs has fostered the utilization of the bacterial homologs for screening and/or synthesis of human metabolites and drug molecules (Gul et al. 2016). Along this line and considering the potential value of FMO-based processes for the production of indigoid pigments (Hsu et al. 2018), the compounds for substrate scope exploration were selected based on the following considerations: trimethylamine is a common endogenous substrate for human FMOs (Krueger and Williams 2005); pyrrole is a probe to test NiFMO activity on heterocyclic organic compounds; methimazole is of pharmacological relevance; indoline, indole, and 6-bromoindole are of

**Fig. 3** Enzymatic activity of NiFMO on selected substrates. The plots show the  $k_{\text{obs}}$  values as a function of substrate concentrations. The activity on each substrate shows Michaelis–Menten behavior. The corresponding apparent steady-state kinetic parameters for the amine substrates are shown in Table 2

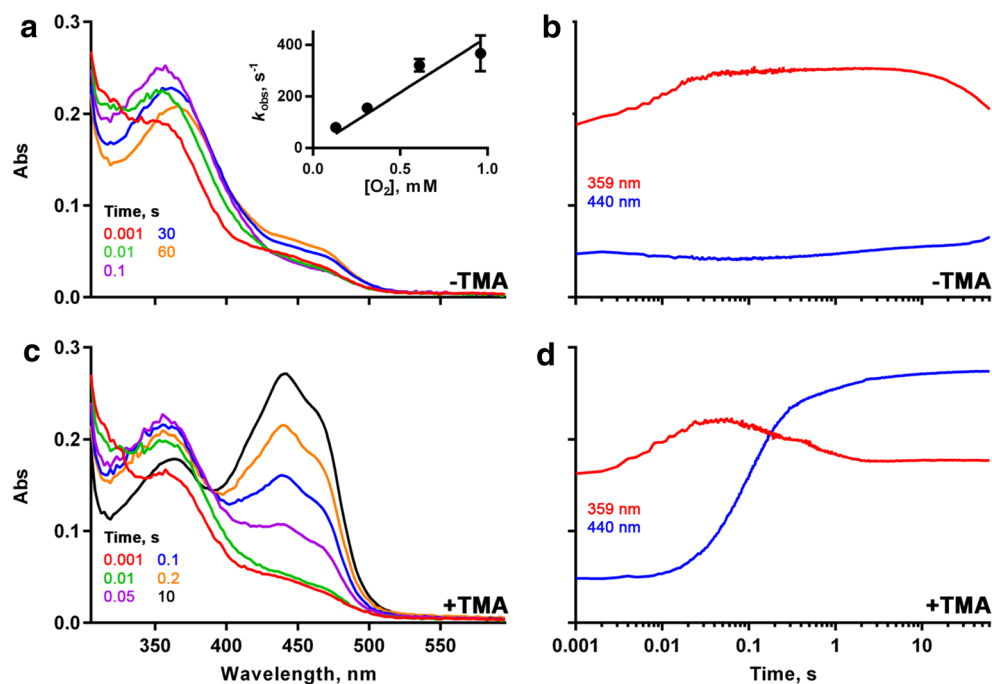


significance for the bio-based synthesis of indigoid pigments. All these compounds proved to be substrates of NiFMO, with trimethylamine exhibiting the highest catalytic efficiency (Table 2). Unexpectedly, enzymatic activity was also observed on tris(hydroxymethyl)aminomethane, initially used as buffer for the enzymatic assays. This shows that

organic buffer components should be used with care when working with enzymes that display a relaxed substrate specificity. Collectively, these data confirm that NiFMO accepts a broad range of *N*-containing molecules, featuring a substrate profile similar to those of mammalian FMOs 1–4.



**Fig. 4** Kinetics of the oxidative half-reaction of NiFMO. Oxidative half-reaction of NiFMO in the absence (a, b) and the presence (c, d) of trimethylamine. Stopped flow spectra and traces were recorded after mixing NADPH-reduced enzyme with a solution containing 0.13 mM dioxygen. To obtain the plot showed in the inset,  $k_{\text{obs}}$  values at various dioxygen concentrations were calculated from exponential fits of the traces at 359 nm



The stopped flow experiments showed that NiFMO has the typical mechanistic features of the flavin-containing monooxygenases and Baeyer-Villiger monooxygenases: efficient reduction by NADPH and fast reaction of the reduced flavin with dioxygen to form a stable C4a-hydroperoxyflavin intermediate. This species efficiently reacts with a substrate to form the oxygenated product (Romero et al. 2018). In the absence of a suitable substrate, the flavin-peroxide slowly decays to form hydrogen peroxide, resulting in a so-called uncoupling activity

(Siddens et al. 2014). The uncoupling for NiFMO is rather slow ( $0.015 \text{ s}^{-1}$ ) preventing the nonproductive usage of NADPH.

As observed for *Methylophaga* FMO, the three-dimensional structure of NiFMO shows a ready-to-react conformation which can expose the reactive FAD-OOH to any suitable nucleophile gaining access to the active site (Fig. 6) (Beaty and Ballou 1981). This reveals how FMOs may exist in the cells in an active form (“cocked gun”) waiting for a suitable substrate with which to react. Substrate selection/accessibility into the active site seems to be mostly guided by the rigid conformation of the crevice leading to it.

From a structure/function point of view, a most relevant observation is that NiFMO features a  $T_m$  value ( $51 \text{ }^\circ\text{C}$ ), which is  $8 \text{ }^\circ\text{C}$  higher than the  $T_m$  of *Methylophaga* FMO ( $T_m$   $43.3 \text{ }^\circ\text{C}$ ) (Formeris et al. 2009). We have comparatively analyzed the crystal structures of NiFMO and *Methylophaga* FMO searching for hints about factors that can enhance thermal stability. The dimeric arrangement of the two proteins is identical in terms of both extension of the dimer interface (about 10% of the monomer accessible surface buried upon dimer formation) and number of intermolecular hydrogen bonds (22 and 24 in NiFMO and *Methylophaga* FMO, respectively). A more significant difference becomes instead apparent from the inventory of the intra-subunit salt bridges which are significantly more numerous in NiFMO (82) than in *Methylophaga* FMO (72). The abundant electrostatic interactions might contribute to thermal stability as previously observed in another flavoprotein monooxygenase (Romero et al. 2016; Vogt et al. 1997).

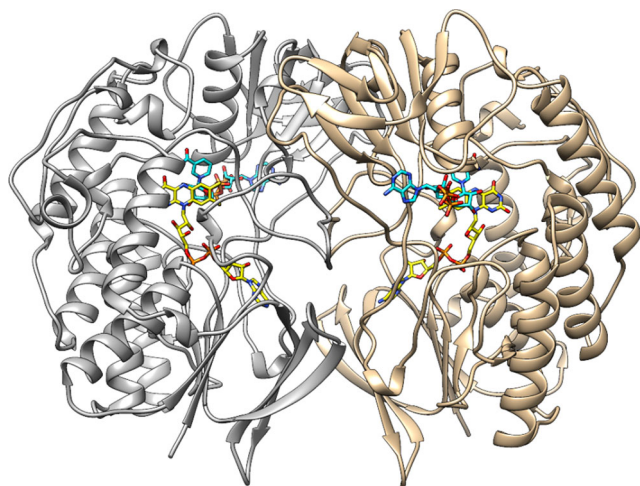


**Fig. 5** Ribbon diagram of the NiFMO crystallographic dimer. Monomers are in gray and light brown. FAD and NADP<sup>+</sup> are depicted with yellow and cyan carbons, respectively. Oxygen atoms are in red, nitrogen atoms in blue, and phosphorous atoms in orange

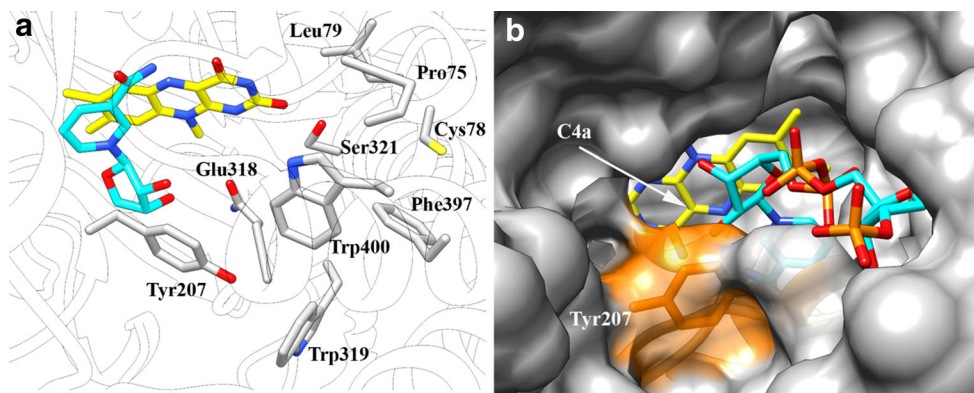


**Fig. 6** The active site of NiFMO. The left panel shows the active site side chains (carbon atoms in gray) together with NADP<sup>+</sup> (carbon atoms in cyan) and FAD (carbon atoms in yellow). The right panel shows surface representation of NiFMO with a view of the catalytic site from the outside. NiFMO displays an open conformation which has the potential to expose the oxygenating flavin-C4a-OO(H) (the “flavin-(hydro)peroxide”) intermediate to any suitable substrate gaining access

In conclusion, here, we report the discovery and characterization of the first thermostable FMO. In view of the ability of this bacterial FMO to oxygenate indigoid compounds as well as a wide variety of substrates converted by typical human FMOs, we believe that NiFMO may take part in bio-based processes targeting both the production of dyes and the preparation of drug metabolites.

**Acknowledgments** We thank Callum R. Nicoll for his help in the project.

**Funding information** Nikola Lončar was supported by the NWO-LIFT project Indigreen. Gautier Bailleul received funding from the European Union’s Horizon 2020 research and innovation program under the Marie Skłodowska-Curie grant Oxytrain, agreement No 722390. The financial support of the Fondazione Cariplo (grant 2015-0406) is acknowledged.

## Compliance with ethical standards

This article does not contain any studies with human participants or animals performed by any of the authors.

**Conflict of interest** The authors declare that they have no conflict of interest.

**Publisher’s Note** Springer Nature remains neutral with regard to jurisdictional claims in published maps and institutional affiliations.

## References

- Alfieri A, Malito E, Orru R, Fraaije MW, Mattevi A (2008) Revealing the moonlighting role of NADP in the structure of a flavin-containing monooxygenase. *Proc Natl Acad Sci U S A* 105:6572–6577. <https://doi.org/10.1073/pnas.0800859105>
- Aliverti A, Curti B, Vanoni MA (1999) Identifying and quantitating FAD and FMN in simple and iron-sulfur-containing flavoproteins. In: Chapman SK, Reid GA (eds) *Methods in molecular biology*, vol. 131: Flavoprotein Protocols, pp 9–23. <https://doi.org/10.1385/1-59259-266-X:9>
- Ameria SP, Jung HS, Kim HS, Han SS, Kim HS, Lee JH (2018) Characterization of a flavin-containing monooxygenase from *Corynebacterium glutamicum* and its application to production of indigo and indirubin. *Biotechnol Lett* 37:1637–1644. <https://doi.org/10.1007/s10529-015-1824-2>
- Beatty NB, Ballou DP (1981) The oxidative half-reaction of liver microsomal FAD-containing monooxygenase. *J Biol Chem* 256:4619–4625
- Cashman JR (2005) Some distinctions between flavin-containing and cytochrome P450 monooxygenases. *Biochem Biophys Res Commun* 338:599–604. <https://doi.org/10.1016/j.bbrc.2005.08.009>
- Cashman JR, Zhang J (2006) Human flavin-containing monooxygenases. *Annu Rev Pharmacol Toxicol* 46:65–100. <https://doi.org/10.1146/annurev.pharmtox.46.120604.141043>
- Cho HJ, Cho HY, Kim KJ, Kim MH, Kim SW, Kang BS (2011) Structural and functional analysis of bacterial flavin-containing monooxygenase reveals its ping-pong-type reaction mechanism. *J Struct Biol* 175:39–48. <https://doi.org/10.1016/j.jbsb.2011.04.007>
- Choi HS, Kim JK, Cho EH, Kim YC, Kim JI, Kim SW (2003) A novel flavin-containing monooxygenase from *Methylophaga* sp strain SK1 and its indigo synthesis in *Escherichia coli*. *Biochem Biophys Res Commun* 306:930–936. [https://doi.org/10.1016/S0006-291X\(03\)01087-8](https://doi.org/10.1016/S0006-291X(03)01087-8)
- Costantini S, Colonna G, Facchiano AM (2008) ESBRI: a web server for evaluating saltbridges in proteins. *Bioinformatics* 3:137–138. <https://doi.org/10.1007/s10529-015-1824-2>
- Dimitriu PA, Shukla SK, Conradt J, Márquez MC, Ventosa A, Maglia A, Peyton BM, Pinkart HC, Mormile MR (2005) *Nitricola lacisaponensis* gen. Nov., sp. nov., a novel alkaliphilic bacterium isolated from an alkaline, saline lake. *Int J Syst Evol Microbiol* 55:2273–2278. <https://doi.org/10.1099/ijs.0.63647-0>
- Dodson EJ, Murshudov GN, Vagin AA (1996) Description of program using maximum likelihood residual for macromolecular refinement, illustrated by several examples. *Acta Crystallogr Sect A: Found Crystallogr* 52:C85–C85. <https://doi.org/10.1107/S0907444911001314>
- Emsley P, Cowtan K (2004) Coot: model-building tools for molecular graphics. *Acta Crystallogr Sect D: Biol Crystallogr* 60:2126–2132. <https://doi.org/10.1107/S0907444904019158>
- Fiorentini F, Geier M, Binda C, Winkler M, Faber K, Hall M, Mattevi A (2016) Biocatalytic characterization of human FMO5: unearthing Baeyer-Villiger reactions in humans. *ACS Chem Biol* 11:1039–1048. <https://doi.org/10.1021/acschembio.5b01016>

- Forneris F, Orru R, Bonivento D, Chiarelli LR, Mattevi A (2009) ThermoFAD, a ThermoFluor-adapted flavin ad hoc detection system for protein folding and ligand binding. *FEBS J* 276:2833–2840. <https://doi.org/10.1111/j.1742-4658.2009.07006.x>
- Gul T, Krzek M, Permentier HP, Fraaije MW, Bischoff R (2016) Microbial flavoprotein monooxygenases as mimics of mammalian flavin-containing monooxygenases for the enantioselective preparation of drug metabolites. *Drug Metab Dispos* 44:1270–1276. <https://doi.org/10.1124/dmd.115.069104>
- Han GH, Bang SE, Babu BK, Chang M, Shin H, Kim SW (2011) Bio-indigo production in two different fermentation systems using recombinant *Escherichia coli* cells harboring a flavin-containing monooxygenase gene (fmo). *Process Biochem* 46:788–791. <https://doi.org/10.1016/j.procbio.2010.10.015>
- Hsu TM, Welner DH, Russ ZN, Cervantes B, Prathuri RL, Adams PD, Dueber JE (2018) Employing a biochemical protecting group for a sustainable indigo dyeing strategy. *Nat Chem Biol* 14:256–261. <https://doi.org/10.1038/nchembio.2552>
- Kabsch W (2010) XDS. *Acta Crystallogr Sect D: Biol Crystallogr* 66:125–132. <https://doi.org/10.1107/S0907444909047337>
- Krissinel E, Henrick K (2007) Inference of macromolecular assemblies from crystalline state. *J Mol Biol* 372:774–797. <https://doi.org/10.1016/j.jmb.2007.05.022>
- Krueger SK, Williams DE (2005) Mammalian flavin-containing monooxygenases: structure/function, genetic polymorphisms and role in drug metabolism. *Pharmacol Ther* 106:357–387. <https://doi.org/10.1016/j.pharmthera.2005.01.001>
- McCoy AJ, Grosse-Kunstleve RW, Adams PD, Winn MD, Storoni LC, Read RJ (2007) Phaser crystallographic software. *J Appl Crystallogr* 40:658–674. <https://doi.org/10.1107/S0021889807021206>
- Orru R, Pazmiño DE, Fraaije MW, Mattevi A (2010) Joint functions of protein residues and NADP(H) in oxygen activation by flavin-containing monooxygenase. *J Biol Chem* 285:35021–35028. <https://doi.org/10.1074/jbc.M110.161372>
- Phillips IR, Shephard EA (2016) Drug metabolism by flavin-containing monooxygenases of human and mouse. *Expert Opin Drug Metab Toxicol* 13:167–181. <https://doi.org/10.1080/17425255.2017.1239718>
- Rioz-Martínez A, Kopacz M, de Gonzalo G, Torres Pazmiño DE, Gotor V, Fraaije MW (2011) Exploring the biocatalytic scope of a bacterial flavin-containing monooxygenase. *Org Biomol Chem* 9:1337–1341. <https://doi.org/10.1039/c0ob00988a>
- Romero E, Castellanos JR, Mattevi A, Fraaije MW (2016) Characterization and crystal structure of a robust cyclohexanone monooxygenase. *Angew Chem Int Ed Engl* 55:15852–15855. <https://doi.org/10.1002/anie.201608951>
- Romero E, Gómez Castellanos JR, Gadda G, Fraaije MW, Mattevi A (2018) Same substrate, many reactions: oxygen activation in flavoenzymes. *Chem Rev* 118:1742–1769. <https://doi.org/10.1021/acs.chemrev.7b00650>
- Siddens LK, Krueger SK, Henderson MC, Williams DE (2014) Mammalian flavin-containing monooxygenase (FMO) as a source of hydrogen peroxide. *Biochem Pharmacol* 89:141–147. <https://doi.org/10.1016/j.bcp.2014.02.006>
- van Berkel WJH, Kamerbeek NM, Fraaije MW (2006) Flavoprotein monooxygenases, a diverse class of oxidative biocatalysts. *J Biotechnol* 124:670–689. <https://doi.org/10.1016/j.jbiotec.2006.03.044>
- Vogt G, Woell S, Argos P (1997) Protein thermal stability, hydrogen bonds, and ion pairs. *J Mol Biol* 269:631–643. <https://doi.org/10.1006/jmbi.1997.1042>
- Winn MD, Ballard CC, Cowtan KD, Dodson EJ, Emsley P, Evans PR, Keegan RM, Krissinel EB, Leslie AG, McCoy A, McNicholas SJ, Murshudov GN, Pannu NS, Potterton EA, Powell HR, Read RJ, Vagin A, Wilson KS (2011) Overview of the CCP4 suite and current developments. *Acta Crystallogr Sect D: Biol Crystallogr* 67:235–242. <https://doi.org/10.1107/S0907444910045749>